JOURNAL OF MATERIALS SCIENCE 25 (1990) 3982–3989

Zirconia toughened cordierite

I. WADSWORTH, J. WANG, R. STEVENS
School of Materials, The University of Leeds, Leeds LS2 9JT, UK

Zirconia–cordierite ceramic composites were fabricated by the hot pressing of cordierite and zirconia powders at 1400° C/20 MPa for 10 min. Both the fracture toughness and fracture strength have been enhanced by the addition of zirconia. Such improvements are due to stress-induced transformation toughening and to the generation of residual stresses. Microcrack toughening has been found not to occur in the composite as a consequence of the large thermal expansion mismatch. The transformability of zirconia inclusions in the cordierite matrix is higher than in the case of an alumina matrix, although the inclusions have a rounded morphology, resulting from the presence of a liquid phase at the hot-pressing temperature.

1. Introduction

Dispersion toughening of oxide ceramics by a zirconia second phase is a well-established process and has been successfully employed to improve the mechanical properties of alumina, mullite and spinel [1–4]. Such toughened ceramics are developed by utilizing toughening mechanisms such as stress-induced transformation toughening, microcracking and crack deflection. As an example, a toughness (K_c) of 10 MPa $m^{1/2}$ and a fracture strength (σ) of 1000 MPa have been obtained from a zirconia-toughened alumina, compared with a fracture toughness of 3 MPa $m^{1/2}$ and a fracture strength of 500 MPa for the single-phase alumina ceramic.

The cordierite system is particularly attractive for enhancement of properties by zirconia additions, because it has many potential applications, arising from its excellent thermal and dielectric properties, but its mechanical properties are poor compared to many engineering ceramics [5–7]. Investigations have been carried out to determine the effects of systematic zirconia additions on the mechanical properties of cordierite. There are essentially two routes by which this can be achieved. The first is to use the glass ceramic process in which zirconia is dissolved in a cordierite melt which is subsequently quenched, to produce a glass supersaturated in zirconia. On heat treatment, precipitation of the zirconia occurs, taking on different morphologies according to the precise conditions used [8–11]. Such precipitation usually occurs in conjunction with devitrification of the glass. The second route involves dispersing zirconia particles in a polycrystalline cordierite powder and either sintering or hot pressing. Pressureless sintering of cordierite to high densities is difficult to achieve due to its narrow sintering range. It can be achieved, however, either by rate-controlled sintering [12] or by debasing [13].

The second route offers improved mechanical properties, but the mechanisms behind these improvements have not been fully investigated. General toughening mechanisms have been used to explain the observed improvements in mechanical properties but the applicability of some of these can be questioned due to the large differences in physical properties existing between cordierite and zirconia. It has been shown that both the differences in physical properties and the chemistry of cordierite affect the transformability of the zirconia and hence the mechanisms of toughening. The transformability of zirconia inclusions in a cordierite matrix would be expected to differ from those in an alumina matrix as a consequence of thermal expansion mismatch and the presence of an amorphous phase at the grain boundaries. Also zirconia is thermodynamically unstable in the cordierite matrix at temperatures above 1280° C due to a reaction resulting in the formation of zircon [14].

The objectives of this work were, therefore, threefold:

(i) fabrication and characterization of zirconia-toughened cordierite;

(ii) a study of the reaction between cordierite and zirconia; and

(iii) a study of the operative strengthening and toughening mechanisms in the system.

2. Experimental procedure

All experimental work was performed on composites fabricated using Baikalox cordierite and Toya Soda zirconia powders.

The mixing of each composition was achieved by ball milling the powders for 24 h in isopropanol, using zirconia media. After homogenization, the isopropanol was rapidly evaporated off by gentle heating on a hot plate. During the drying process, the slurry was vigorously stirred to prevent differential settling. The dried powders were consolidated by hot pressing in an inductively heated graphite die, 25 mm diameter, for 10 min at 1400° C under a pressure of 20 MPa.

After fabrication, density measurements were made using the water displacement method to verify that complete densification had occurred. Strength measurements were made on bars machined from the pressed discs using a four-point bend rig (outer span

0022–2461/90 $03.00 + .12 © *1990 Chapman and Hall Ltd.*

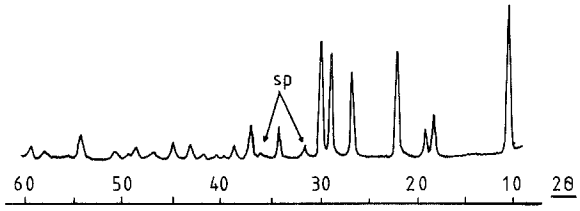

Figure 1 X-ray diffraction trace (Cu$K\alpha$) of the as-received cordierite powder (sp = spinel).

20 mm, inner span 6 mm) in an Instron 1185 testing machine at a cross-head speed of 0.5 mm min^{-1}. Fracture toughness was measured by the micro-indentation method using a Zwick diamond indentor with an applied load of 3 kg. Characterization of the microstructure and fracture behaviour was performed by means of Hitachi HS700 and Camscan Series 4 SEMs and a Jeol 200CX TEM.

3. Results and discussion

3.1. Phase identification

Inspection of the X-ray diffraction trace for the as-received cordierite powder indicated the presence of small amounts of spinel (Fig. 1). Further investigation by STEM and EDX microanalysis confirmed this to be the case (Fig. 2). Amorphous material and mullite were also detected in the as-received powder and the hot-pressed material (Fig. 3). The presence of these additional phases was believed to be due to the production route used for the manufacture of the powder. The process involved a two-stage calcination of ammonium alum, magnesia and pyrolytic silica, resulting in an estimated 85% conversion to cordierite.

Although the formation of zircon is predicted at temperatures in excess of 1280° C [14], X-ray analysis of the hot-pressed composites revealed neither the presence of zircon nor an increase in the amount of spinel present (Fig. 4). Extensive micro-analysis also failed to locate any reaction product of zirconia and cordierite. It was believed that at the processing temperatures used, the reaction kinetics were insufficiently fast to produce any evidence of a reaction over the 10 min the material was held at temperature.

To confirm this hypothesis, samples containing 20 vol % ZrO_2–3 mol % Y_2O_3 were aged for varying times at 1350° C for up to 10 h. The results of the X-ray analysis are shown in Fig. 5. As can be seen, after 1 h, a small peak due to zircon formation was seen at 27° (2θ). These results agree with those of Nieszery *et al.* [12] who used rate-controlled sintering with the final stage involving a dwell at 1400° C for 1 h to produce dense cordierite/zirconia composites. Further ageing resulted in only a marginal increase in the zircon peak height.

It may, therefore, be concluded that the reaction between cordierite and zirconia is thermodynamically possible but kinetically slow under the conditions described.

3.2. Transformability of zirconia in cordierite

The transformability of zirconia inclusions in a cordierite matrix is unexpectedly high. As shown in Table I, approximately 50% of the zirconia grains in the ZrO_2–3 mol % Y_2O_3 undergo transformation on cooling from the hot-pressing temperature. This result is very different from the results obtained for ZTA where 100% tetragonal zirconia is retained with greater than 2 mol % yttria as a stabilizer [15, 16]. Moreover, it was

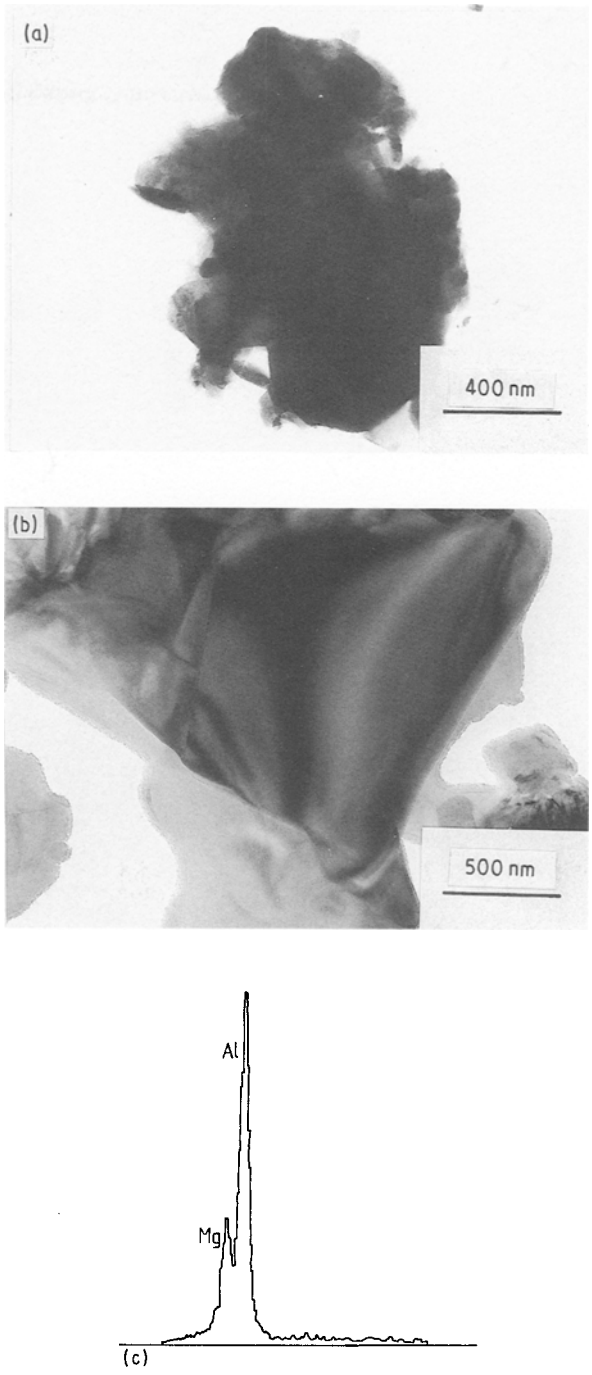

Figure 2 Transmission electron micrographs of spinel in (a) the as-received powder, (b) the hot-pressed composite; (c) shows the EDX trace recorded.

TABLE I Tetragonal phase content in the hot-pressed cordierite–zirconia composites determined on the polished and ground surfaces

Stabilizer (mol %)	% Tetragonal (polished)	% Tetragonal (ground)
2.0	28	12
2.5	42	20
3.0	50	27

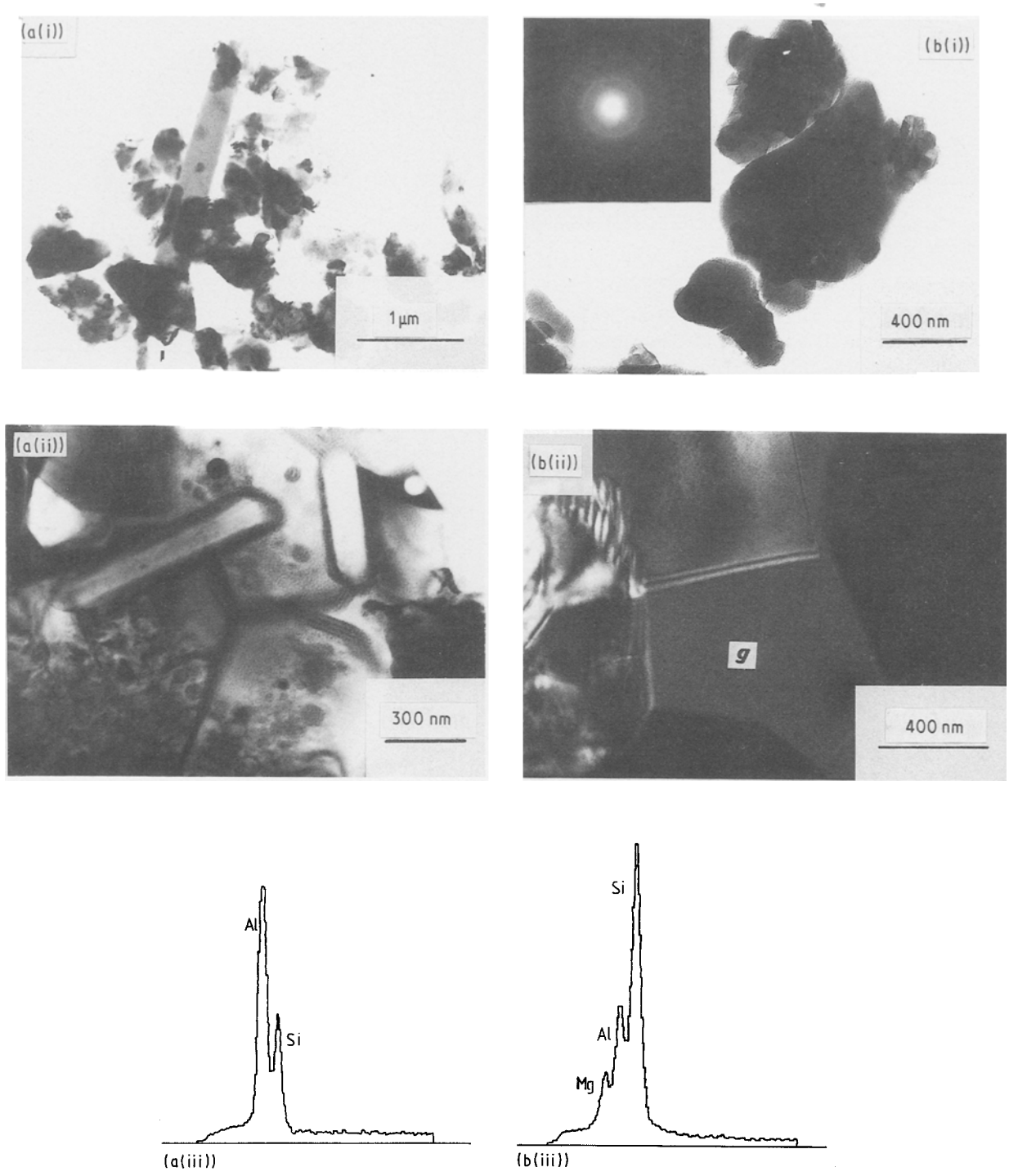

Figure 3 (a) Transmission electron micrographs with accompanying energy dispersive spectroscopic trace showing mullite in (i) the as-received powder, (ii) the hot-pressed cordierite–zirconia composite. (b) Transmission electron micrographs with accompanying energy dispersive analysis of X-rays trace showing glass in (i) the as-received powder, (ii) the hot-pressed cordierite–zirconia composite.

observed that destabilization increased with increasing time at the hot-pressing temperature. Using the equation developed by Garvie and Nicholson [17], the change in the percentage of tetragonal present due to ageing at 1350° C for various times is given in Table II.

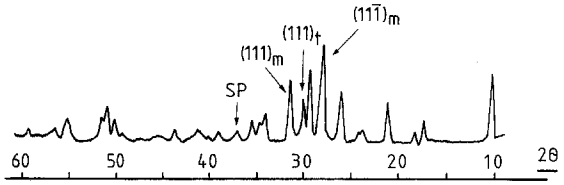

Figure 4 X-ray diffraction trace for cordierite–20 vol % ZrO_2–2 mol % Y_2O_3 indicating the major tetragonal (t) and monoclinic (m) zirconia peaks and no apparent increase in spinel.

There are several well-established parameters which affect the transformability of zirconia inclusions including: (1) zirconia particle size, (2) zirconia grain morphology, (3) stabilizer content, (4) matrix constraint.

TABLE II Change in tetragonal phase content with ageing time at 1350° C in the hot-pressed cordierite–zirconia composite

Ageing time (min)	% Tetragonal
10	28
60	12
300	11

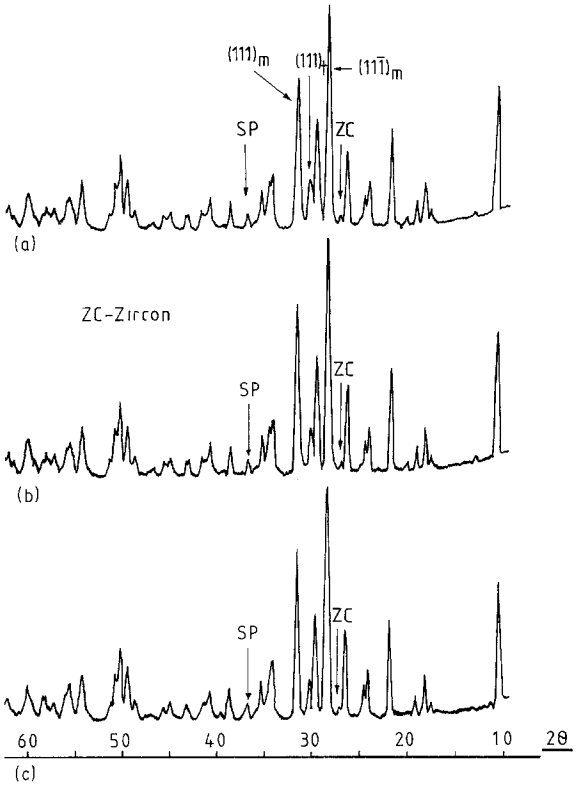

Figure 5 X-ray diffraction traces for cordierite–20 vol % ZrO_2–3 mol % Y_2O_3 aged at 1400° C for (a) 1 h, (b) 5 h, (c) 10 h.

3.2.1. Particle size

It is commonly accepted that the transformability of particles of the tetragonal zirconia phase increases with increasing size. The high stability of a small tetragonal zirconia grain can be considered, thermodynamically, to be due to the reduced surface energy, which is part of the overall free energy [18]. Therefore the tetragonal zirconia phase is thermodynamically stable when its size is small, less than a critical value. Kinetically, the instability of a large tetragonal grain is due to the increased presence of monoclinic nuclei as a consequence of an increased number of defects in the structure [19–21]. The zirconia inclusions in the cordierite matrix in this work are considered to be small, below the critical size, as a result of the low hot-pressing temperature (1400° C) when compared with sintering temperatures for zirconia-toughened alumina ceramics. It is, therefore, to be expected that the transformability of the zirconia inclusions in the cordierite would be lower than that of those in the zirconia-toughened alumina ceramics as a consequence of a smaller grain size. However, the experimental results in Table I show that this is not the case.

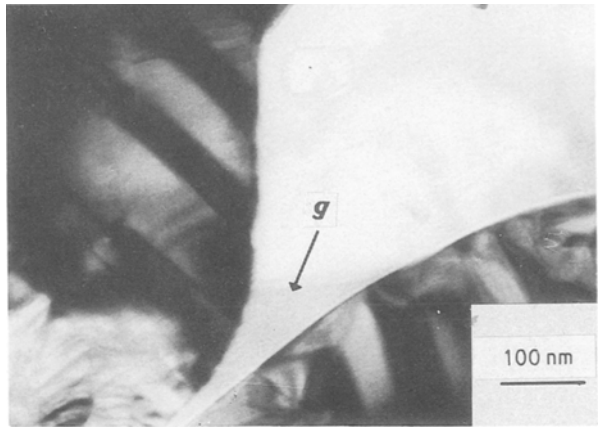

Figure 7 Amorphous phase at a triple point of zirconia and cordierite grains.

The possibility of grain growth at elevated temperatures due to Ostwald ripening also needs to be considered. Such a process would occur as a result of zirconia/yttria dissolution into the amorphous phase, diffusion through it and reprecipitation on other larger zirconia grains. However, if this was to occur, and there is no evidence in the form of an increase in zirconia particle size to suggest that it does, much of the yttria dissolved in the amorphous phase would not

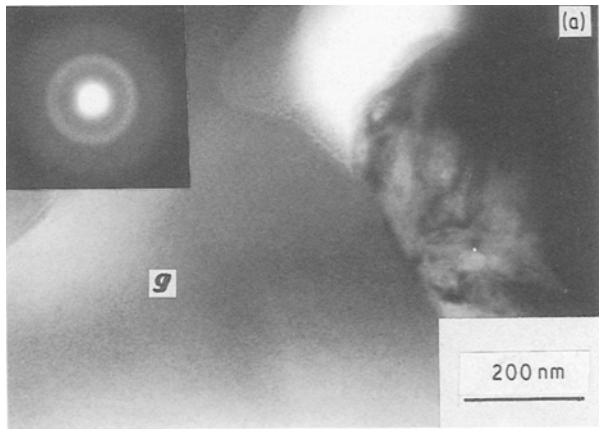

Figure 6 Zirconia inclusions in a cordierite matrix. Note their rounded morphology and the absence of matrix microcracking.

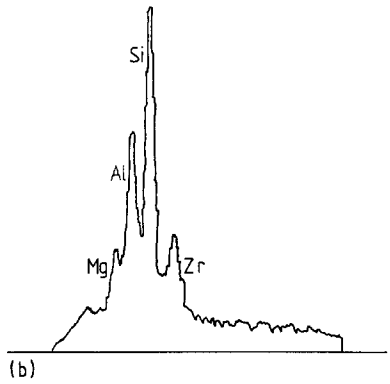

Figure 8 (a) Amorphous region similar to that illustrated in Fig. 3b but in this case adjacent to a zirconia grain. (b) The associated energy dispersive analysis of X-rays trace clearly indicating the presence of zirconia.

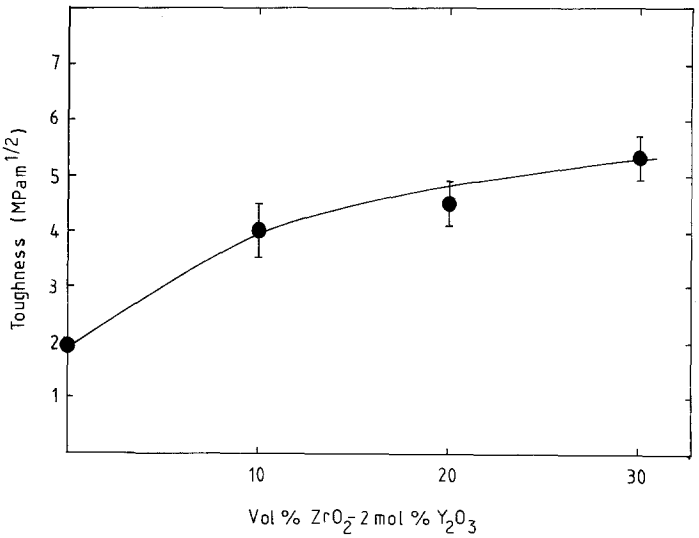

Figure 9 The effect of ZrO_2–2 mol % Y_2O_3 additions on the fracture toughness of cordierite–zirconia composites.

reprecipitate as the quantities present in solution would be below the saturation level. Thus any growth of the zirconia particles would result in yttria deficiency in the newly deposited zirconia, resulting in greater transformability of the tetragonal particles.

3.2.2. Grain morphology

An angular grain exhibits higher transformability as a consequence of increased surface energy of the tetragonal phase and the energetically more favourable nucleation of the monoclinic phase [19–21]. It may be seen in Fig. 6 that the zirconia inclusions in a cordierite matrix are less angular than those in an alumina matrix due to the presence of a liquid phase present at the zirconia grain boundaries (Fig. 7). This suggests that zirconia inclusions in a cordierite matrix are likely to be less transformable as a consequence of their shape. This is clearly not the case, as the experimental results indicate, although it is likely that the transformability has been reduced somewhat as a result of the zirconia grain morphology. However, a more dominant process is operative and the net effect is an increase in transformability of the zirconia.

3.2.3. Yttria loss

The alloying element content in zirconia is perhaps the most critical parameter in determining transformability. From the phase diagram for the ZrO_2–Y_2O_3 system [22] it is known that 3 mol % yttria is sufficient to achieve a fully stable tetragonal solid solution, the critical size for the tetragonal to monoclinic transformation increasing sharply in the 2 to 3 mol% yttria range. However, as shown in Table I, only 50% of the tetragonal phase is retained in composites consisting of 20 vol % ZrO_2–3 mol % Y_2O_3. This result is of particular interest because it eliminates increased grain growth of the zirconia as a cause of transformation due to the very short times used to densify the composites. The work performed by Cheng and Thompson [9] revealed that the solubility of zirconia in cordierite glass is approximately 10 wt %. Dissolution of zirconia into the silicate phase in this system was also confirmed. Fig. 8 shows a transmission electron micrograph of an amorphous region adjacent to a zirconia grain. Microanalysis revealed the presence of zirconia within this phase. It was not possible to detect changes in the yttria content due to the low overall concentrations present. The problem was compounded by the overlap of Zr$K\alpha$ and Y$K\alpha$ peaks which necessitated the study of the much lower intensity L emissions.

The amorphous phase illustrated in Fig. 7 is noticeably darker than the adjacent cordierite grain, suggesting that it is less transparent to electrons possibly

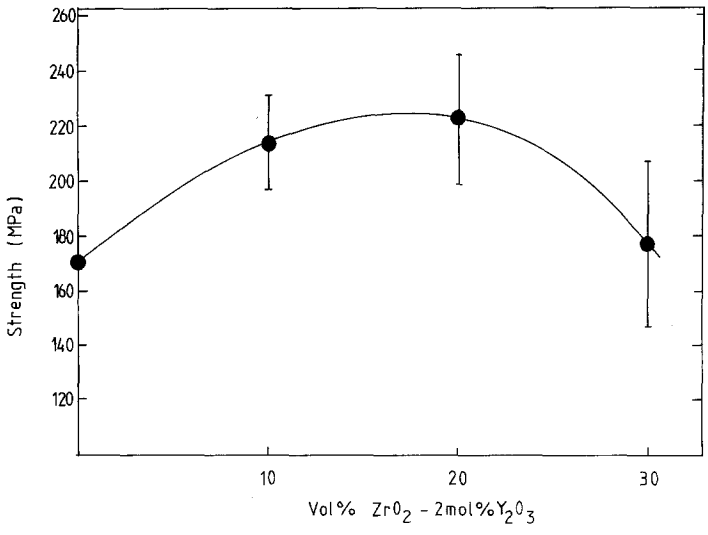

Figure 10 The dependence of fracture strength on ZrO_2–2 mol % Y_2O_3 content in cordierite–zirconia composites.

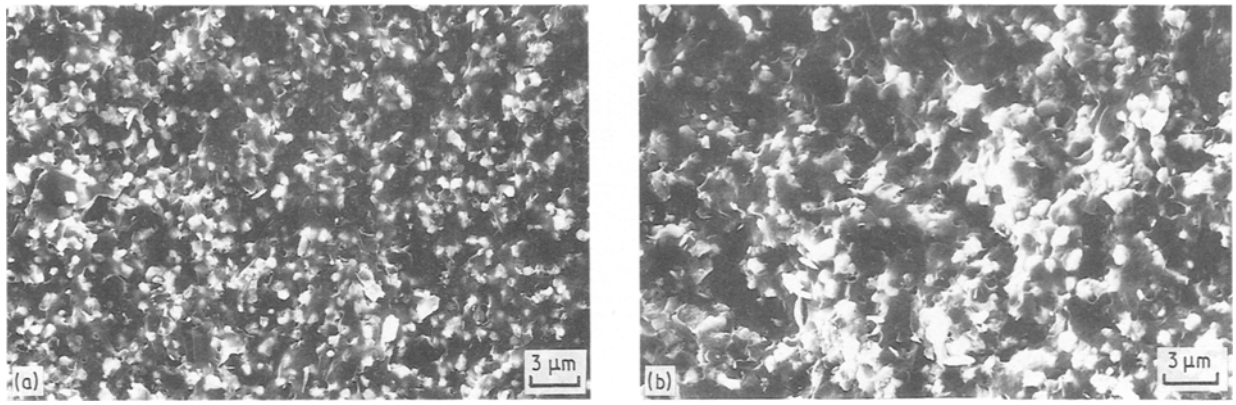

Figure 11 Fracture surfaces of (a) cordierite–10 vol % ZrO_2–2 mol % Y_2O_3, (b) cordierite–30 vol % ZrO_2–2 mol % Y_2O_3.

as a result of the presence of elements of higher atomic mass such as zirconium and yttrium. The similarity in ionic radii of Zr^{4+} and Y^{3+} (79 pm and 89 pm, respectively) would suggest that diffusional loss of yttria may occur.

3.2.4. Matrix constraint

The constraint exerted on the zirconia particles by cordierite is lower than that exerted by alumina as a consequence of the large difference in thermal expansion coefficient and lower elastic modulus. The lower thermal expansion of cordierite, compared with that of zirconia, leads to tensile stresses being imposed on the zirconia grains during cooling from the fabrication temperature. The presence of such tensile stresses will favour transformation. The differential shrinkage due to thermal expansion mismatch can be calculated from Equation 1 below

$$e = 3(\alpha_c - \alpha_z)\Delta T \quad (1)$$

in which α_c and α_z are linear thermal expansion coefficients for cordierite and zirconia and were taken as 2 and 10 MK^{-1}, respectively. Thus a relative volume contraction of 3.0% is expected for zirconia on cooling from the fabrication temperature, if ΔT is assumed to be 1200° C.

It has been widely accepted that both stress-induced transformation toughening and transformation-induced microcrack toughening are related to the volume expansion associated with the tetragonal to monoclinic transformation. In the case of zirconia-toughened alumina composites, the volume contraction associated with the thermal expansion mismatch due to cooling from the fabrication temperature is much smaller than the volume expansion associated with the transformation. Therefore, both stress-induced transformation and microcrack toughening can occur, depending on such parameters as solute oxide content and zirconia particle size. However, the situation is different in zirconia-toughened cordierite composites in that the volume contraction associated with the thermal expansion mismatch is directly comparable to the volume expansion associated with the tetragonal to monoclinic transformation. It is therefore apparent that the volume expansion associated with the transformation will be compensated by the thermal expansion mismatch.

TEM observations revealed that microcracking did not occur around the transformed monoclinic zirconia inclusions (Fig. 6) indicating mutual cancellation of elastic strains developed by the two processes. The results, given in Table I, do indicate that the matrix does prevent about 50% transformation in all the composites, suggesting that the cordierite imposes a certain degree of constraint on the zirconia grains. It is suggested that microcrack toughening is not an important mechanism in the cordierite–zirconia composites, even though a high percentage of zirconia

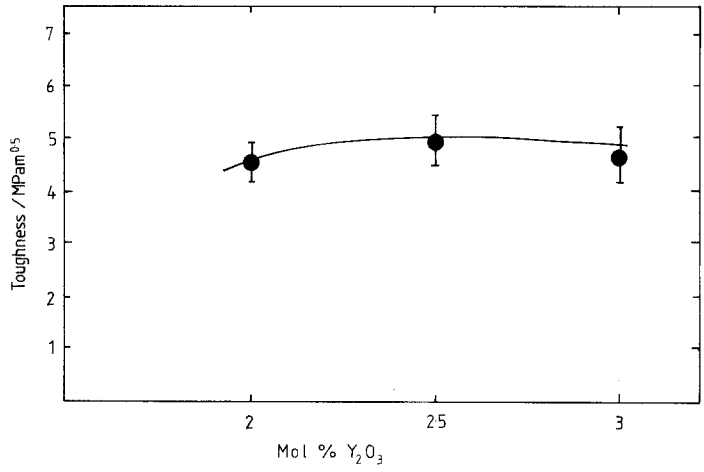

Figure 12 The dependence of fracture toughness on yttria content in cordierite–zirconia composites.

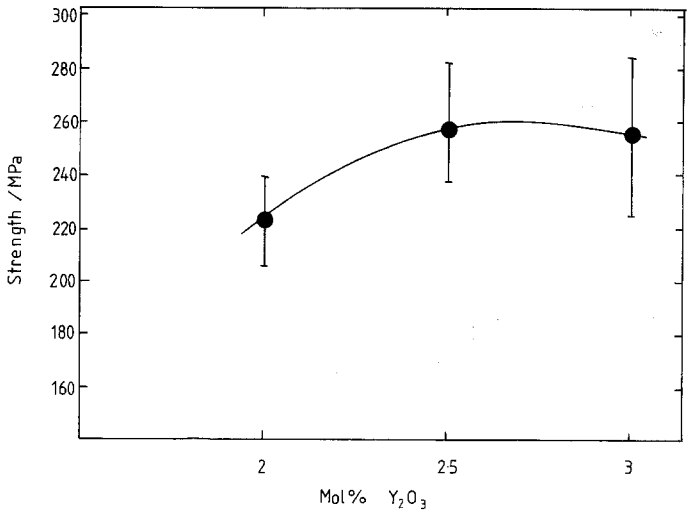

Figure 13 The dependence of fracture strength on yttria content in cordierite–zirconia composites.

grains transformed to the monoclinic form on cooling from the hot-pressing temperature.

3.3. Fracture toughness and fracture strength

Fig. 9 shows the indentation toughness as a function of the volume fraction of ZrO_2–2 mol % Y_2O_3 in the cordierite matrix. It can be seen that the fracture toughness increases with increasing zirconia content. A fracture toughness, $K_c = 4\,MPa\,m^{1/2}$, is obtained when 10 vol % ZrO_2 is introduced into the cordierite matrix, compared with $1.9\,MPa\,m^{1/2}$ for the monolithic material.

Fig. 10 shows the four-point bend strength as a function of zirconia content. Unlike the relationship between the fracture toughness and zirconia content, the strength shows a maximum at 20 vol % ZrO_2–2 mol % Y_2O_3. However, the specimen containing 30 vol % ZrO_2–2 mol % Y_2O_3 shows a large reduction in fracture strength. Fracture strength is related to the microstructure of the composites. The Griffith equation [23] relates two parameters which determine the fracture strength of brittle materials, the fracture energy and critical flaw size. As is seen from Figs 9 and 10, the variation in fracture strength and fracture toughness are not coincident. The critical flaw size in the composite containing 30 vol % ZrO_2–2 mol % Y_2O_3 is required to be much larger than for the specimens containing less zirconia. Fig. 11 shows a scanning electron micrograph of the fracture surfaces of composites containing 10 and 30 vol % ZrO_2–2 mol % Y_2O_3, respectively. Dispersion of zirconia inclusions in the cordierite matrix is more homogeneous in the specimen containing 10 vol % ZrO_2–2 mol % Y_2O_3 than in the composite containing 30 vol % ZrO_2–2 mol % Y_2O_3 where zirconia agglomerates of 10 to 15 μm exist in the latter. Moreover, flaws are to be seen at the interface between the agglomerates and the matrix. It may, therefore, be concluded that the reduction in fracture strength for the specimen containing 30 vol % ZrO_2–2 mol % Y_2O_3 is due to the heterogeneous dispersion of zirconia inclusions, even though it exhibits an increased toughness.

Another factor which influences the fracture strength of the composites is the grain growth of the matrix. It would be expected that grain growth is inhibited with increasing zirconia additions as a result of grain-boundary pinning. A slight transition from transgranular fracture to intergranular fracture was observed in the cordierite as a result of adding 30 vol % ZrO_2–2 mol % Y_2O_3. Fig. 12 shows the indentation toughness as a function of yttria content in the zirconia inclusions for the composites containing 20 vol % partially stabilized zirconia. The fracture toughness increases sharply with yttria content up to 2 mol % but levels off from 2 to 3 mol %. The result differs from the relationship between the fracture toughness and yttria content observed in zirconia-toughened alumina, in which a maximum toughness occurs at 2 mol % yttria. This difference is considered to be due to the destabilization of the zirconia in cordierite composites. The transformability of zirconia inclusions, as measured by X-ray diffraction, originally containing 2.5 to 3 mol % yttria in the cordierite, is similar to that of those containing 2 mol % yttria in alumina.

Fig. 13 shows the four-point bend strength as a function of yttria content for the same specimens as shown in Fig. 12. The fracture strength shows a similar trend to the fracture toughness, indicating that there is no change in critical flaw size in the specimens as a result of varying the yttria content of the zirconia.

As discussed earlier, microcrack toughening is not considered to be responsible for the mechanical property improvement in zirconia–cordierite composites as a result of the large thermal expansion mismatch of the two phases. Observation of cracks around indentations demonstrated that the degree of crack deflection by zirconia inclusions was also very limited (Fig. 14). Two mechanisms are thus considered to be important in toughening and strengthening of zirconia–cordierite composites in the present work: stress-induced transformation toughening and the presence of residual stresses.

4. Conclusions

An investigation of fabrication, microstructure and mechanical properties of zirconia-toughened cordierite composites has been made. Zirconia inclusions can be retained up to 1350° C without any substantial reaction with cordierite, although destabilization due

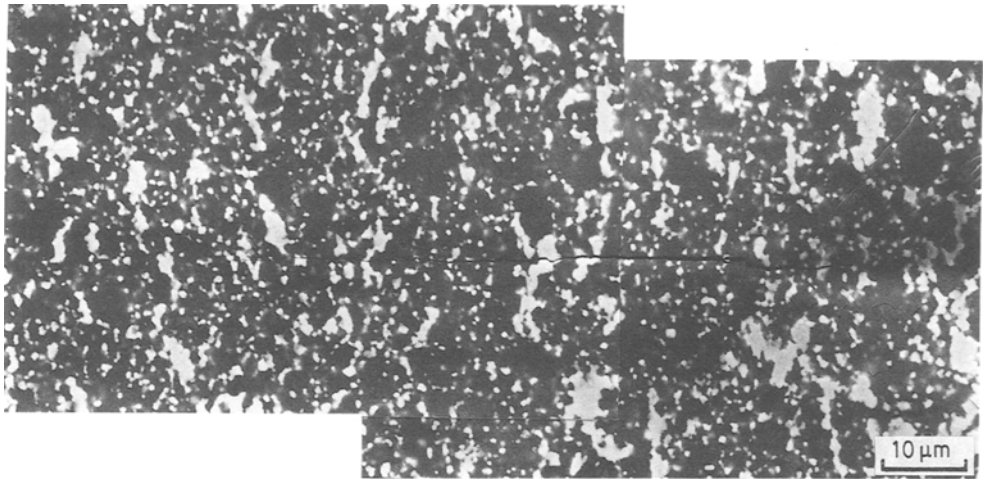

Figure 14 Scanning electron micrograph of an indentation-derived crack in cordierite–20 vol % ZrO_2–2 mol % Y_2O_3.

to yttria loss is suspected. The evidence to support this belief is as follows.

1. High proportions of monoclinic zirconia were observed in the as-pressed composites, suggesting that grain growth is not responsible for destabilization.

2. Destabilization increases with prolonged ageing at elevated temperature, suggesting that the process is time dependent thus ruling out the lack of matrix constraint being the cause of destabilization.

3. The experimental results confirm that zirconia dissolves in the residual glass. Hence, it would be expected that dissolution of yttria would also occur. The retained zirconia inclusions have a rounded morphology, as a consequence of the presence of a liquid phase at sintering temperature. The transformability of zirconia inclusions in the cordierite matrix is higher than in an alumina matrix as Y_2O_3 leaching is thought to take place. Both the fracture toughness and fracture strength are enhanced by the addition of zirconia inclusions. The mechanisms accounting for these improvements include stress-induced transformation toughening and residual stress generation. Microcracks have not been found in cordierite–zirconia composites although a large percentage of the zirconia inclusions transform to the monoclinic form on cooling from the sintering temperature. This is explained on the basis that the volume expansion associated with the tetragonal to monoclinic transformation is partially compensated by the thermal mismatch strains developed on cooling from the fabricating temperature.

References

1. N. CLAUSSEN, in "Advances in Ceramics", Vol. 12. Science and Technology of Zirconia II, edited by N. Claussen, M. Ruhle and A. H. Heuer (The American Ceramic Society, Columbus, Ohio, 1984) p. 325.
2. A. G. EVANS and R. M. CANNON, *Acta Metall.* **35** (1986) 761.
3. N. CLAUSSEN and J. JAHN, *J. Amer. Ceram. Soc.* **63** (1980) 228.
4. Y. KUBOTA and H. TAKAGI, in "Advances in Ceramics", Vol. 24. Science and Technology of Zirconia III, edited by S. Somiya, N. Yamamoto and H. Yanagida (The American Ceramic Society, Westerville, Ohio, 1988) p. 999.
5. T. I. BARRY and R. MORRELL, *Proc. Brit. Ceram. Soc.* **22** (1973) 27.
6. R. MORRELL, "Handbook of Properties of Technical and Engineering Ceramics" (H.M.S.O., London, 1985).
7. C. R. GOSTELOW and J. E. RESTALL, *Proc. Brit. Ceram. Soc.* **22** (1973) 117.
8. B. H. MUSSLER and H. W. SHAFER, *Amer. Ceram. Soc. Bull.* **64** (1985) 1459.
9. Y. CHENG and D. P. THOMPSON, *Proc. Brit. Ceram. Soc.* **42** (1989).
10. M. McCOY, W. E. LEE and A. H. HEUER, *J. Amer. Ceram. Soc.* **69** (1986) 292.
11. M. McCOY and A. H. HEUER, *ibid.* **71** (1988) 673.
12. K. NIESZERY, K. L. WEISSKOPFF, G. PETZOW and W. PANNHORST, in "High Technology Ceramics", edited by P. Vincenzini (Elsevier, Amsterdam, 1987) p. 841.
13. R. MORRELL, *Proc. Brit. Ceram. Soc.* **28** (1979) 53.
14. P. G. HEROLD and W. J. SMOTHERS, *J. Amer. Ceram. Soc.* **37** (1954) 353.
15. S. HORI, M. YOSHIMURA and S. SOMIYA, *ibid.* **69** (1986) 169.
16. J. WANG and R. STEVENS, *J. Mater. Sci.* **23** (1988) 804.
17. R. C. GARVIE and P. S. NICHOLSON, *J. Amer. Ceram. Soc.* **55** (1972) 303.
18. F. F. LANGE, *J. Mater. Sci.* **17** (1982) 225.
19. A. H. HEUER and M. RUHLE, in "Advances in Ceramics", Vol. 12. Science and Technology of Zirconia II, edited by N. Claussen, M. Ruhle and A. H. Heuer (The American Ceramic Society, Columbus, Ohio, 1984) p. 1.
20. I. W. CHEN and Y. H. CHAIO, *Acta Metall.* **31** (1983) 10.
21. *Idem, ibid.* **33** (1985) 1827.
22. H. G. SCOTT, *J. Mater. Sci.* **12** (1977) 311.
23. A. A. GRIFFITH, *Phil. Trans. R. Soc. (London)* **221A** (1921) 163.

Received 2 June
and accepted 17 October 1989